

## DAMIC: Dark Matter In CCD

R. GAIOR

*Laboratoire de Physique Nucléaire et de Hautes Energies (LPNHE), Universités Paris 6 et Paris 7,  
CNRS-IN2P3, Paris, France*



DAMIC is a direct detection dark matter experiment using thick silicon CCDs as target and sensor. This technique is sensitive to nuclear recoil induced by the interaction of low mass WIMP on the target nucleus thanks to the silicon crystal characteristics and low noise readout capabilities. DAMIC is installed at SNOLAB and has set limits on WIMP-nucleon cross section between 1 and 20 GeV/c<sup>2</sup> with a detector of 9 grams cumulating an exposure of 0.6 kg·day. After explaining the functioning and the advantages of the technique we will review the performances and results of the DAMIC detector and the status of the current upgrade to DAMIC100. We will also focus on the challenges and the potential of a prospective versions of a kg scale detector.

### Introduction

DAMIC is a detector based on cooled CCD used as a DM direct detector and sensitive to WIMP mass below 20 GeV/c<sup>2</sup>. The technique was first considered in the years 2010<sup>1</sup>. We will show in this contribution that since then, many efforts were undertaken and rewarded by competitive limits in the WIMP search at low mass.

After a short explanation of the detection general functioning, we will detail the calibration and background studies done for the DAMIC operation. The analysis carried out with 0.6 kg·day exposure are then presented as well as the search for hidden photon, another DM candidate, in the range from 1.2 to 30 eV. The currently installed version the setup called DAMIC100 will be described and the future generation, DAMIC1K is discussed.

### 1 The DAMIC detector

**Detection principle** The DAMIC sensor is a semiconductor crystal in silicon N-doped. It is divided in pixels, and acts as the target but as the detector as well. As an energy deposit occurs in the CCD, electron-hole pairs are created at a rate of one pair per 3.77eV deposited and dragged to the surface of the CCD by an electric field. Charges are then stored in potential wells in a 1  $\mu$ m thick layer on the surface. After the exposition of the CCD, the pixels are read out and an *image* of the energy deposits during the time of the exposition is obtained. A WIMP particle

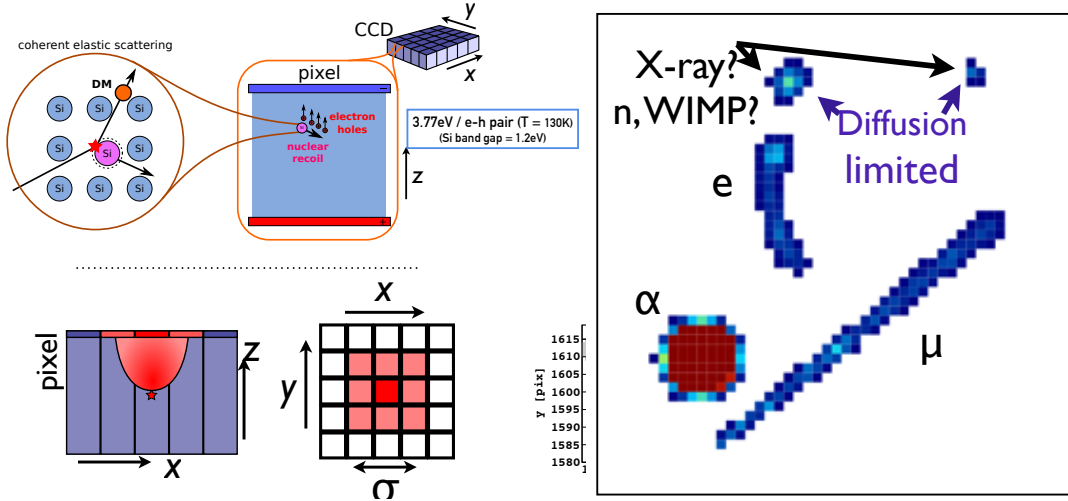


Figure 1 – Left: sketch of the functioning of the DM detection with CCD; bottom: sketch of the charge spread during the diffusion of the pixel surface. Right: Example of particle signal in a CCD. Characteristics features for  $e^-$ ,  $\nu$ ,  $\alpha$ ,  $\beta$  can be clearly noticed.

would scatter on the silicon nuclei and induce a nuclear recoil which in turn would produce a small energy deposit as sketched in the Figure 1-top left. The energy threshold for the electron hole pair production of the Silicon as well as a low reading noise translates in a low WIMP mass threshold. Furthermore, as sketched on the Figure 1-bottom left, the charges are directed along the z axis and diffused on the x and y axis so the RMS of the charge distribution at the surface  $\sigma_{xy}$  is an estimator of the depth of the interaction, giving a 3D reconstruction of the energy deposit location. The figure 1-right illustrates the particle identification capabilities of the CCD technology based of their characteristic features.  $\alpha$  particle are clearly distinguished by the large and located energy deposit, electron are more scattered and yield a wormy like track and while muon passes through and produce a straight track.

DAMIC CCDs are three-phase polysilicon gate structure with a buried p-channel based on a technology developped for DECam CCD<sup>2</sup>. They are 0.675 mm thick and the low density of donors ( $10^{11}/cm^3$ ), allows for a large depletion zone with a relatively low voltage ( 40V). A CCD is composed of  $4k \times 2k$  or  $4k \times 4k$  pixels, and weight 2.9g or 5.8g. Each pixel is a square of  $15 \mu m$  side and provides a signal almost unpolluted by dark current (less than  $10^{-3} e^-/\text{pixel/day}$  at 120 K).

The read out of the CCD is carried out after each exposition, typically of 8 hours for the DM search run. The charges are transferred from one row to the next one with a parallel clock, while a higher frequency serial clock transfers the electrons of the last row to the output node where the charge is measured. The operation of charge measurement adds an electronic noise, however the uncertainty on the measured number of charges is as low as to 1.8 thanks to correlated double sampling technique. This sets the detection threshold to low energy, around 50eVee (electron Volt electron equivalent).

The acquisition can be operated in two modes,  $1 \times 1$  and  $1 \times 100$ . In the former case, every pixel is read and saved offering the best spatial resolution, whereas in the latter case, 100 rows are transferred in the last one before its serial transfer to the output node leading to a better energy resolution at the cost of a poorer spatial resolution.

**The DAMIC detector** The DAMIC detector is installed at the SNOLAB underground facility, in the Vale's Creighton nickel mine. It is located below of 2 km of rock, or 6010 meter water equivalent. The DAMIC CCDs are enclosed in a series of containers which are shown in the Figure 2. Going from the most inner part, each CCD lays on a silicon support, is held in a copper frame and is connected to a flex cable to form a module ( Fig 2-a ) . The module is

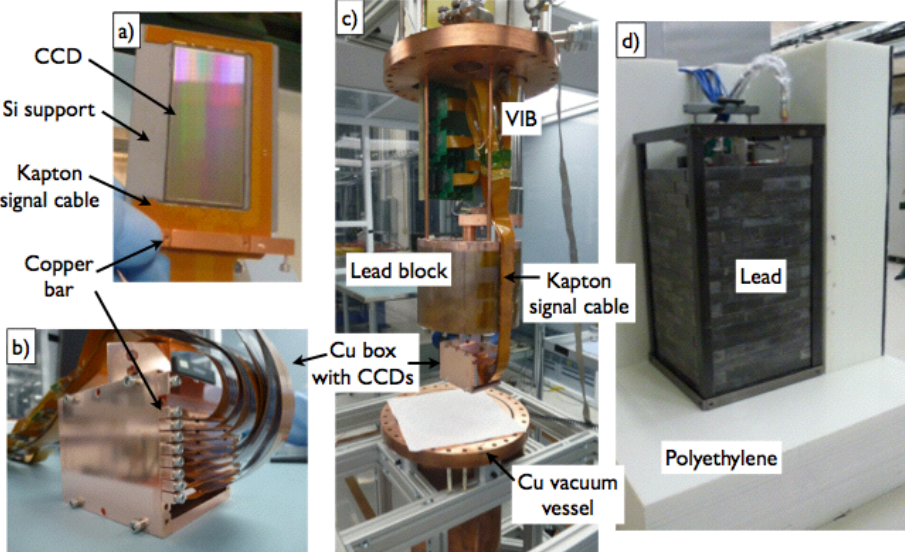


Figure 2 – Views of the DAMIC detector including its shielding. See text for details.

inserted in one slit of a copper box ( Fig 2-b ) . The box is placed in a copper vessel, under a lead block ( Fig 2c ) and put under a very low pressure of  $10^{-6}$  mbar and cooled down to a temperature of 120 K. The vessel is surrounded by a lead castle of 21 cm thickness to shield the sensitive part against  $\gamma$  rays. Note that the lead layer close to the vessel was selected from ancient lead, poor in  $^{210}Pb$  contaminant. Finally a 42 cm high density polyethylene shield acts as a neutron absorber( Fig 2-d ) .

**Energy calibration** The CCD technology also has the advantage of showing a good linearity en energy. The response of DAMIC CCD to source of photons of known energy is shown in Figure 3-left. X-rays sources are chosen down to energies of around 1keVee and optical sources are used to cover the lower energy region where DAMIC is still sensitive. The linearity factor is constant to 5% error over the three order of magnitudes. Additionally, the Fano factor  $F$ , that enters in the energy resolution definition as  $\sigma_E \propto \sqrt{E \cdot F}$  is found to be 0.13. As a WIMP particle is expected to produce a nuclear recoil, the detector needs to be calibrated to such process. The Figure 3-right shows the relation between the ionization energy and the nuclear recoil energy. It was performed on a silicon detector with a fast neutron source above 2 keVr in the study<sup>4</sup> and on a CCD similar to the DAMIC one with photoneutron at lower energy<sup>5</sup>.

**Background** A crucial point in low rate experiment is the background contamination. The DAMIC experimental technique has no discrimination power of a nuclear recoil as expected for a WIMP signal from an electron recoil, as produced by low energy  $\beta$  or Compton. Hence, the background limitation and control is of prime importance. While the detector is well shielded from the neutron induced by atmospheric muons with 6km w.e. of rock, it can be polluted by radioactive contaminants in the shielding, the components around the sensor, or even within the sensor itself. A special care is given in the handling of the CCD and the nearest part of it. The copper is etched and most of the material are screened to verify the low radioactive contamination. Inner most lead layer are made out of ancient lead batch to ensure a low activation by cosmic rays. A nitrogen flux is circulated around the vessel to limit the radon concentration close to the sensor. Additionally, thanks to the combined spatial and energy resolution specific to DAMIC, the contamination from some radioactive chain can be measured by correlating event position and energy with their expected features. Radioactive contamination

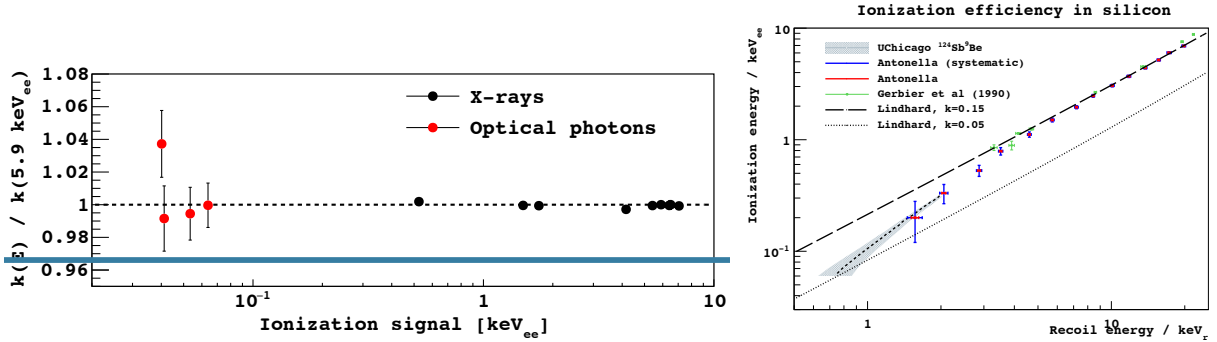


Figure 3 – Left: Energy calibration of DAMIC CCD with electronic recoil signal (or ionization energy). Right: Relation between nuclear recoil energy and ionization energy.

can also take place inside the bulk of Silicon. The <sup>32</sup>Si isotope is produced via spallation of argon in atmosphere and is found in the Silica used to extract the Silicon. The  $\beta$  decay of <sup>32</sup>Si leads to <sup>32</sup>P and could induce a low energy background. The study of events compatible spatially, in energy and in time with the decay chain parameters (the beta spectrum and the half time) is carried out to estimate the <sup>32</sup>Si concentration. The Figure 4-left shows the evolution (each curve represent a stage of DAMIC) of the background in DAMIC detector over the years. It shows an impressive decrease from  $10^4$  d.r.u. = counts / keV / day / kg to 5 d.r.u. thanks to the changes along the years including the improvements detailed in this paragraph.

## 2 Dark Matter searches

**Low mass WIMP search** After a period mainly dedicated to background studies and reduction (years 2013-2015), DAMIC setup has acquired data for DM search in 2015<sup>6</sup>. The data are composed of 1x1 and 1x100 acquisition with 2 and 3 CCDs of 8 Mpixels and 2.9 g each. Exposure are either  $10^4$  or  $3 \times 10^4$  s and the average background event rate below 10 keVee over the data taking period is 30 d.r.u..

The images are first treated to remove the unstable pixels: after a correction for the pedestal and the correlated noise observed as a systematic shift in the two output node serving for the reading, the pixels with too large and frequent variations from their normal condition are masked. Furthermore, since a blank image is acquired for each exposed image, the consistency of the distribution between the exposed and blank images serves as a last check before the event selection.

Below 10 keVee, nuclear recoil induced by a WIMP is expected to leave a very little ionization energy in the detector. Hence, the event search is directed toward pointlike events. A mask is constructed on each image to exclude clusters, i.e. contiguous pixels with signal larger than 4 times the electronics noise and with a total energy larger than 10 keVee. To find clusters, the image is scanned with a  $11 \times 11$  pixels sliding window. In each of these windows, the likelihood of 2D white noise ( $L_N$ ) and of a white noise plus a Gaussian signal with a fixed width ( $L_G$ ) are computed and compared. If  $-(\ln \frac{L_G}{L_N}) \leq -4$ , the window is selected and then the signal is fitted to find the best parameters to describe the cluster. The distribution of  $\Delta LL = -\ln(\frac{\max(L_G)}{L_N})$  is compared with simulated ionization events and blank image. Candidate events are selected with the condition of  $\Delta LL \leq -28$  in the case of 1x1 data. At this point further selection is operated to exclude spatially correlated events which can originate from pixel defect if they are at the same location on different images, or from radiation following radioactive decay when the separation distance is less than  $300 \mu\text{m}$ . The distribution of the candidate events is displayed in Figure 4 in the energy as a function of  $\sigma_{xy}$  plane. A final selection is applied to remove surface event likely to be produced by low energy electrons emitted from the surface directly

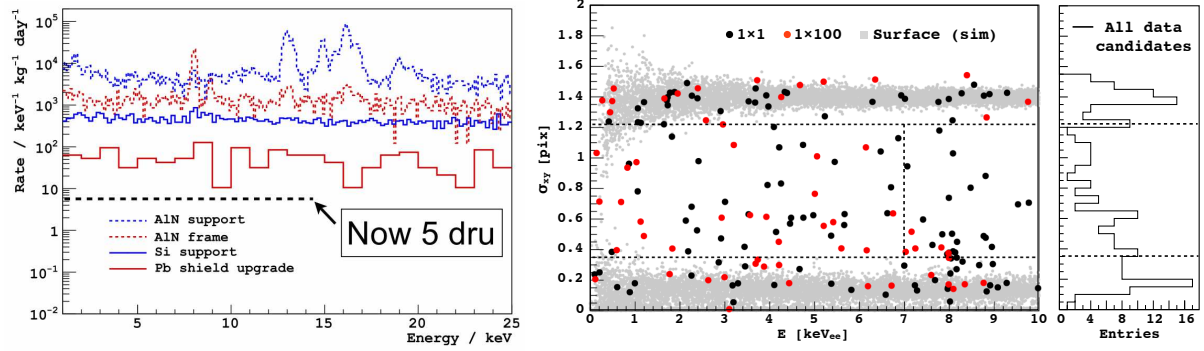


Figure 4 – Left: Evolution of the background in the DAMIC detector. The current level has reach 5 d.r.u. Right: Distribution of selected events for the WIMP search in the plane energy as a function of  $\sigma_{xy}$ , the depth estimation.

surrounding the CCD. Additionally the excess found at 8 keVee from the copper fluorescence line is also excluded. The number of final candidates inside the fiducial area (inside the dashed rectangle in the Figure 4) amounts to 31 for  $1 \times 1$  mode and 23 for the  $1 \times 100$  mode.

WIMP induced event and the electrons produced by Compton scattering inside the fiducial volume are indistinguishable individually. However, while for the WIMP induced signal one expects an exponentially decreasing spectrum, it is expected flat for the Compton background. Hence we construct the following likelihood function with the energy of each candidate event:

$$L_{s+b}(s, b, M|E) = e^{-(s+b)} \times \prod_{i=1}^N [s f_s(E_i, M) + b f_b(E_i)] \quad (1)$$

where  $s$  and  $b$  are the expected number of signal and background events,  $f_s$  and  $f_b$  their energy distribution. Note that  $f_s$  depends on the mass of the WIMP and the model assumed. We assume the standard halo parameters: galactic escape velocity of  $544 \text{ km.s}^{-1}$ , most probable galactic WIMP velocity of  $220 \text{ km.s}^{-1}$ , mean orbital velocity of Earth with respect to the Galactic center of  $232 \text{ km.s}^{-1}$ , and local dark matter density of  $0.3 \text{ GeV c}^{-2} \cdot \text{cm}^{-3}$ . Upper limits on the WIMP nucleon elastic scattering cross section are constructed by scanning the WIMP mass parameter. For each mass  $M$  assumed, we produce a set of Monte Carlo samples with a defined number  $s$  of signal events according the assumed spectrum  $f_s$ . We compare the likelihood of the data with the distribution found in the MC sample and search the mass  $M_\chi$  and cross section  $\sigma_{\chi-n}$  for which we reject the initial hypothesis with 90% confidence level. The limits retrieved in the plane  $(M_\chi / \sigma_{\chi-n})$  are displayed in Figure 5(black solid line). It shows that DAMIC is competitive in the low mass region  $E < 10 \text{ GeV}$ . For the first time a region of the CDMS-II potential signal (blue region in the Figure 5) is excluded with the same target composition.

**Hidden photon** Aside from the WIMP hypothesis, light bosonic candidate has been proposed as DM candidate. Semiconductor like DAMIC detector are sensitive to eV scale hidden photon via their absorption in the Silicon crystal. The absorption in a medium can be express with the effective mixing parameter related to the photo electric cross section. The absorption of hidden photons in DAMIC CCD would yield a very small signal but would modify the expected distribution of pixel content. Such a signature was searched in 6.5 d of data of one CCD, chosen for its low leakage current and measured during a dedicated run at lower temperature than usual operations (105 K). The data are compared with simulation of hidden photon absorption and limits on the kinetic parameter and the mass of the hidden photon were placed. They are the most stringent direct detection limit between 3 and  $12 \text{ eV.c}^{-2}$ <sup>7</sup> (see Figure 5).

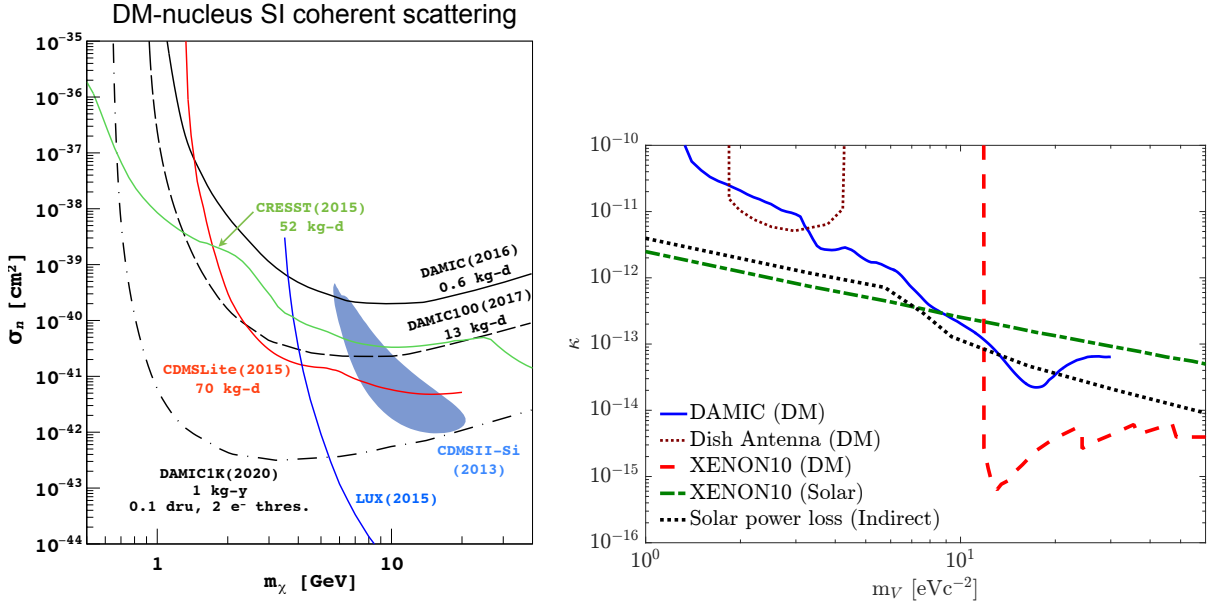


Figure 5 – Left: Limits on WIMP cross section as a function of the WIMP mass imposed by DAMIC detector. Right: Limits on the kinetic mixing parameter of the hidden photon.

### 3 DAMIC100 and beyond

**DAMIC100** An extension of the DAMIC setup has been installed in April 2016 and January 2017. The new setup is currently composed of seven  $4\text{k} \times 4\text{k}$  CCD (5.9g each) for a total mass of 41 g. Several other changes were carried out. The copper box and some modules were replaced. A part of the shielding was also replaced with Roman ancient lead.

**Toward DAMIC1K** A next generation experiment with a mass of 1 kg is also considered for the near future. Additionally to an increase of mass, DAMIC1K will attempt to reduce the background noise and decrease the energy threshold to explore lower WIMP mass with a better sensitivity. The expectation in terms of sensitivity are presented in Figure 5-left (dotted-dashed line) for 1 kg.year, and 0.1 d.r.u.. Lowering the electronics noise would shift this curve to lower mass.

However, to scale up the detector mass by around one order of magnitude can present some challenges. With the current CCDs, one would require 180 CCDs to reach 1 kg. Keeping the current technology, a few changes would decrease this number. For instance, for a size of individual CCD raised to  $6\text{k} \times 6\text{k}$  and the thickness increased to  $\sim 1$  mm, the number of required CCDs drops to around 50. Further developments in the CCD fabrication process could even increase the thickness to a few mm.

As far as the background noise is concerned, the current DAMIC installation noise is stable. Full simulations of the radioactive contamination are being carried out to understand further the origin of the current background to later reduce it and optimize the shielding or the geometry of the future detector. Since the irreducible background will eventually come one from the CCD bulk contaminant such as  $^{32}\text{Si}$  and  $^{3}\text{H}$ , the process of fabrication and transportation might have to be controlled as well. Finally, work to decrease the readout noise is under progress. Several options, sometimes complementary are considered: the optimization of the first amplification stage; the use of skipper CCD (these devices under development allow the multiple reading of a pixel without any noise addition); finally a digital filtering of the CCD signal would help in a more precise determination of the charge of each pixel.

## Conclusion

The DAMIC detector, a CCD based dark matter detector was described. The calibration carried out down to very low ionization energy and the measurement of its equivalent in nuclear recoil energy were presented. The effort to reduce the background to finally reach stable operation with 5 d.r.u. were also shown. Thanks to these improvements DAMIC has been shown to be a competitive detector in the low mass region with the limits placed with 0.6 kg.day of data. Further improvements are ongoing with the recent installation of DAMIC100 and the development of the next generation of 1kg scale detector DAMIC1K.

## References

1. DAMIC Collaboration, *Phys.Lett. B*711 (2012) 264-269.
2. S. Holland, D. Groom, N. Palaio, R. Stover, and M. Wei, *IEEE Trans. Electron Devices* 50, 225 (2003).
3. B. L. Flaugher et al., *Proc. SPIE Int. Soc. Opt. Eng.* 8446, 844611 (2012).
4. F. Izraelevitch *et al.*, *Journal of Instrumentation* **12**, P06014 (2017)
5. B. J. Scholz, A. E. Chavarria, J. I. Collar, P. Privitera, and A. E. Robinson *Phys. Rev. D* **94**, 122003 (2016)
6. DAMIC Collaboration, *Phys. Rev. D* **94**, 082006 (2016).
7. DAMIC Collaboration, *Phys. Rev. Lett.* **118**, 141803 (2017).